Systems & Control Transactions

Research Article - Peer Reviewed Conference Proceeding
ESCAPE 35 - European Symposium on Computer Aided Process Engineering
Ghent, Belgium. 6-9 July 2025
Jan F.M. Van Impe, Grégoire Léonard, Satyajeet S. Bhonsale,
Monika E. Polańska, Filip Logist (Eds.)

PSE PRESS

Systematic design of structured packings based on shape optimization

Alina Dobschall*, Elvis Michaelis, and Mirko Skiborowski

Hamburg University of Technology, Institute of Process Systems Engineering, Hamburg, Germany
* Corresponding Author: alina.dobschall@tuhh.de.

ABSTRACT

Distillation is not only a widely-used but also an energy-intensive separation process, in which internals such as structured packings play an important role. Increasing mass transfer efficiency by designing improved structured packings in order to provide a large interfacial area while enabling low pressure drop is one promising approach to quickly reduce the energy requirements of vacuum distillation where low pressure drop is important for separation efficiency and thermal stability of the processed media. The current work presents an innovative method to optimize structured packings by means of constrained shape optimization on the basis of computational fluid dynamics simulations to minimize the pressure drop while maintaining a constant specific surface area. To solve the fluid dynamic optimization problem, a gradient-based local optimization algorithm in a continuous adjoint formulation is utilized. The shape optimization is applied for a commonly used Rombobak packing, and tested as a refinement method for an initial structure derived by topology optimization. The results demonstrate a successful reduction of the pressure drop in both cases, which can be attributed to several factors, including the refinement of the edges and the mending of the dead zones.

Keywords: structured packings, CFD simulation, optimization-based design

INTRODUCTION

The design of structured packings for thermal separation columns has been the subject of extensive research for 60 years [1]. Despite the profound expertise and considerable advances that have already been gained in this field, it remains a challenging but promising task. This is due to the fact that the packing performance depends on a variety of fluid dynamic and mass transfer-related parameters, which exert a mutual and not necessarily beneficial influence on one another. The systematic development of improved packings by means of computational fluid dynamics (CFD) simulations is a promising approach to yield improved designs that can be manufactured on the basis of the derived computer aided design (CAD) models.

Various research groups conducted parameter variations of specific structured packings based on CFD simulations to systematically generate new improved designs [2,3]. However, only a limited number of studies have employed mathematical optimization for this purpose. While Lange and Fieg [4] focused on the optimization of novel structures by means of topology optimization based on CFD simulations, Blauth et al. [5] performed shape optimization of a specific structured packing that was initially derived from the Rombopak 9M packing [6]. In the topology optimization approach [4], the material distribution is varied in a predefined grid structure making use of an evolutionary algorithm. While this approach provides high potential for innovation, it can only produce rough design drafts for tractable grid sizes. In contrast, shape optimization modifies a given structure gradually based on gradient information of the objective function, as obtained through adjoint simulations [7]. This approach does not allow for the generation of new structures, but can be beneficial as a refinement tool for further improvement of existing packing designs or initial course structures. As demonstrated and experimentally validated by Blauth et al. [5], the shape optimization has been proven to be successful, resulting in an increased separation efficiency of 20%.

In this contribution, shape optimization coupled with

single-phase CFD simulations of the gas phase is used to improve two initial packing structures. By starting from a topology-optimized packing structure, the sequential integration of both optimization methods is evaluated, while the shape optimization approach is further tested for an established structured packings on the basis of an initial Rombopak packing.

METHODOLOGY

The initial structures of the two different packing elements are depicted in Figure 1, showing the topology-optimized packing [4] and the Rombopak packing. The individual structural elements of the topology-optimized packing (left) consist of cubes. Due to the sharp edges, they exert a detrimental impact on the overall flow such that vortex formation can occur here, which are associated with increased pressure drop. The Rombopak packing (right) consists of thin, x-shaped structural elements, which are already significantly more conducive to the flow. The size of the packings to be optimized is a single packing element at laboratory scale with a diameter of 54 mm diameter and a height of 100 mm selected based on the dimensions of an available experimental setup to measure the fluid dynamics.

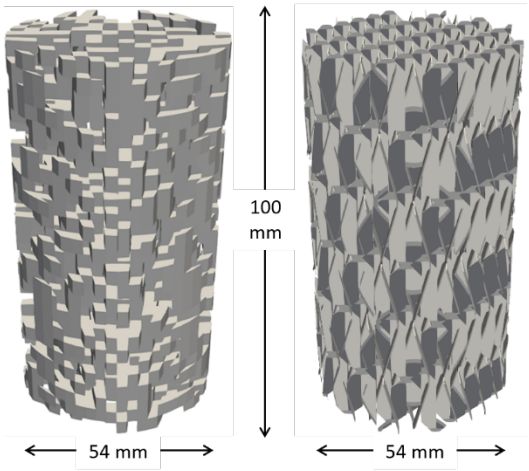

Figure 1. Initial packings for shape optimization: topology-optimized packing (left) and Rombopak packing (right).

CFD simulations

To evaluate the pressure drop of the different packings generated during shape optimization, CFD simulations are performed using the software OpenFOAM. The fluid flow through the packings is modelled based on the continuity equation and the Navier Stokes equations. Whereas the primary focus of this study is on the fluid dynamics, the specific surface area serves as a simplified metric for the potential interfacial area for mass transfer, assuming a completely wetted packing surface. While this assumption is certainly optimistic it allows to use simple single-phase simulations instead of a complex multiphase model, which is important for the complex optimization task. The air flow is entered at the bottom of the packing with a velocity of 0.2 m/s, corresponding to an F-factor of 0.22 $Pa^{0.5}$. At these conditions, the flow can be assumed as incompressible. Further assumptions for the CFD simulations include steady state and laminar flow. Newtonian fluid behavior is be assumed and the flow is modeled at ambient pressure and temperature. The domain includes the packing element surrounded by a hollow cylinder representing the column wall. For convergence reasons, the cylinder is enlarged to a diameter of 63.5 mm. Furthermore, the length of the cylinder exceeds that of the packing on both sides to effectively simulate the inlet and outlet areas of the fluid. To solve the CFD simulations, the SIMPLE algorithm is used. The pressure drop is evaluated over the inlet and outlet of the computational domain. Furthermore, post-processing tools are employed to calculate the specific surface area of the structured packing, which is defined as the ratio of the surface area to the volume. To execute shape optimization, an additional solver is used, which is described in the following section.

Adjoint-based shape optimization

The shape optimization problem can be stated as

$$\min J(\boldsymbol{u}, p, \boldsymbol{\beta}) \; s.t. \, \boldsymbol{h}(\boldsymbol{u}, p, \boldsymbol{\beta}) = 0 \wedge g(\boldsymbol{\beta}) = 0 \qquad (1)$$

with the objective function J describing the pressure drop Δp, $\boldsymbol{h}$ corresponding to the mathematical model of the fluid dynamics problem, consisting of the continuity and the Navier Stokes equations, as well as a geometric constraint g, which keeps the specific surface area a constant. The design variables $\boldsymbol{\beta}$ of the optimization algorithm are defined as the surface points of the packing, which form the faces and thereby the shape of the packing. The surface points can be moved along the surface normal during the optimization in order to deform the packing in a targeted manner for minimizing the objective function.

A gradient-based local optimization algorithm in a continuous adjoint formulation is used to solve the fluid dynamic optimization problem [7]. An overview of the iterative process of shape optimization is depicted in Figure 2. The initial geometry is provided in the form of a stl file and is meshed before the optimization of the current iteration starts.

To obtain information about the extent for shifting the surface points, the gradients are necessary, which are also referred to as sensitivities in this context. An effective method for calculating the sensitivities with a large number of design variables, as in this case, is the adjoint method. In addition to the conventional system of equations based on the continuity equation and the

Navier Stokes equations, referred to as primal equation system, a similarly structured adjoint equation system is set up. This second system is a purely mathematical construct. To solve the constrained optimization problem of equation 1, the Lagrange method is applied. The resulting Lagrange function is shown in equation 2, where Ω corresponds to the solution domain of the fluid dynamic problem and the Lagrange multipliers are represented by the adjoint velocity $\boldsymbol{u_a}$ and the adjoint pressure p_a.

$$L = J + \int (\boldsymbol{u_a}, p_a) \boldsymbol{h} d\Omega \tag{2}$$

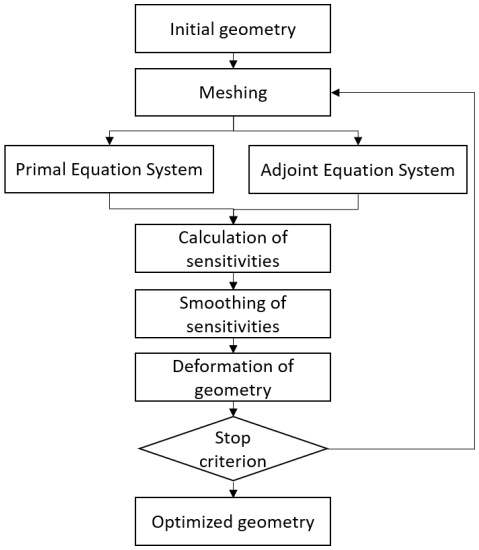

Figure 2. Schematic visualization of the iterative process of shape optimization.

The sensitivity field with respect to the design variables can then be calculated from the scalar product of the wall-normal gradients of the primary and adjoint velocities:

$$\frac{\partial L}{\partial \boldsymbol{\beta}} = -\nu (\boldsymbol{n} \cdot \nabla) \boldsymbol{u_a} \cdot (\boldsymbol{n} \cdot \nabla) \boldsymbol{u} \tag{3}$$

The geometrical constraint of a constant specific surface area is implemented using a penalty method whereby a penalty term weighted with a penalty parameter γ is added to the sensitivity values as illustrated in equation 4. The specific surface area of the initial packing is denoted by a_0 and the lower limit for the specific surface area a_{min} is defined as a_0 subtracted by a tolerance value of 1.5 m²/m³ for both packing types. In order to prevent uncontrolled expansion of the structural elements, which leads to a decrease in the free cross-sectional area and thus to an increase in pressure drop, all negative sensitivities are set to zero once the geometric constraint is violated. Consequently, the correction of the sensitivity field is constrained to positive sensitivities.

$$\frac{\partial L}{\partial \boldsymbol{\beta}_{corrected}} = \frac{\partial L}{\partial \boldsymbol{\beta}_{>0}} + \gamma \frac{a_{min} - a}{a_0} \tag{4}$$

Subsequent to the calculation of the sensitivity values, a smoothing equation with a specified number of iterations can be used in order to reduce the scatter of the sensitivity field. Depending on the specific application, the magnitude of the sensitivity field varies, which can result in complications, such as overlapping faces when using the deformation tool. To address this, the sensitivities are normalized to the largest value. For the deformation of the surface points, the method of steepest descent with a specified step size α is applied. As indicated by equation 5, the surface normal displacement of the packings' surface points is obtained by multiplying the step size by the negative gradient of the surface sensitivities, which indicates the search direction.

$$\boldsymbol{\beta}^{i+1} = \boldsymbol{\beta}^{i} + \alpha \left(-\frac{\partial L}{\partial \boldsymbol{\beta}}^{i} \right) \tag{5}$$

The iterative shape optimization continues as the deformed geometry is used as a new initial packing in the next iteration step. The process continues until a specified stop criterion is reached.

In order to ensure that the cylindrical shape of the structured packing is retained and that it can be stacked in height without gaps, a maximum volume is introduced and sensitivities on the outer surfaces of the packing in this volume are set to zero. This approach also provides a constant cylindrical reference volume for the calculation of the specific surface area, thereby ensuring the comparability of the packings across different iterations of shape optimization.

The success of shape optimization is subject to the selection of the previously outlined hyperparameters, for which the values selected on the basis of preceding preliminary studies are shown in Table 1. For both structured packings, a step size of 10^{-4} is used whereas a higher penalty parameter and no smoothing iterations are used for the Rombopak packing compared to the topology-optimized packing for ensuring the specific surface area to remain above the prescribed lower limit.

Table 1. Selected parameters for the shape optimization algorithm

Parameter	Topology-optimized packing	Rombopak packing
Step size	10^{-4}	10^{-4}
Penalty parameter	10,000	100,000
Smoothing iterations	10	0

RESULTS

The shape optimization results are first discussed for the topology-optimized packing and subsequently for the Rombopak packing, analyzing the development of the pressure drop and specific surface area, as well as the deformation of the packings induced by shape

optimization and the respective velocity plots and streamlines.

Topology-optimized packing

Figure 3 shows the progression of shape optimization regarding pressure drop and specific surface area over the course of the iterations. For the initial packing, the pressure drop is 0.063 mbar/m and the specific surface area of the packing is 375.3 m^2/m^3. It should be noted that the pressure drop is relatively low, which is a consequence of the low F-factor. As the number of iterations increases, the pressure drop decreases continuously. In the first 20 iterations, the decline is precipitous, followed by a more modest decrease that is almost stagnating in the last 10 iterations. The specific surface area is characterized by a fluctuating course over the iterations. It decreases until the defined lower limit of 373.8 m^2/m^3, is attained, at which point the geometric constraint becomes effective. After the 136th iteration, the minimum limit for the specific surface area is permanently undercut, so that the optimum is found at this point. The pressure drop of this packing is 0.053 mbar/m and the specific surface area 374.0 m^2/m^3. Overall, the pressure drop is reduced by 16% during the process of shape optimization while the specific surface area is kept constant with minor deviations of 0.3%

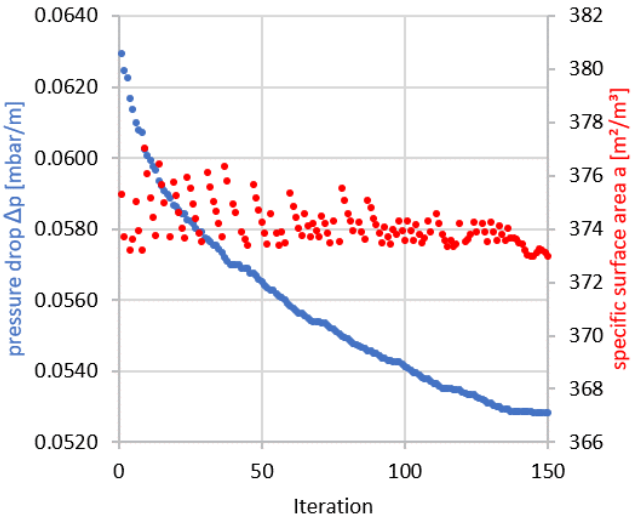

Figure 3. Shape optimization results of the pressure drop and specific surface area for the topology-optimized packing.

In order to conduct a more thorough examination of the effect of shape optimization, a comparison is made between the initial packing and the optimized packing shown in Figure 4. It becomes evident that the initially cubic structural elements are rounded, as expected, and extended in the direction of the flow. This results in a reduction in pressure drop, attributable to the gentler deflection of the fluid flow. Moreover, a reduction in horizontal surfaces is evident subsequent to shape optimization. In a distillation column, this phenomenon is anticipated to result in diminished stagnant liquid and a more frequent renewal of the liquid film, thereby enhancing mass transfer. A more detailed analysis of the two zoomed-in sections in Figure 4 offers additional insights. The section is situated at the bottom of the packing, with the cube in the center representing a dead zone since it is only open at the bottom. The figure demonstrates that this zone is filled with material during shape optimization, a factor that exerts a positive influence on both the pressure drop and the distribution of the fluid.

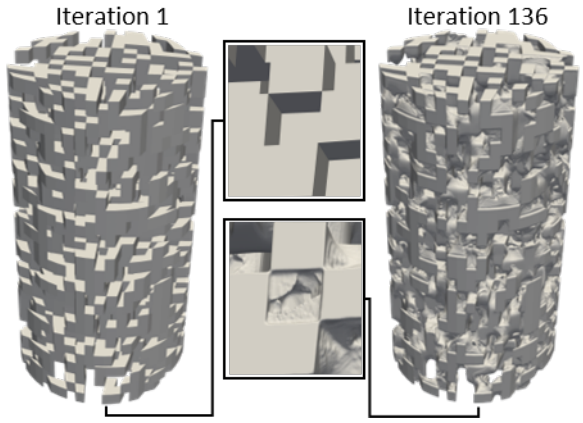

Figure 4. Packing element of the initial topology-optimized packing and after 136 shape optimization iteration steps including zoomed-in sections at the bottom of the packing.

To analyze the effects of the deformations on the fluid dynamics, sections of the velocity plots and the streamlines in Figure 5 are considered, where the initial packing and the optimized packing of iteration 100 are compared. For both cases, it is evident that subsequent to entering the packing from the bottom at 0.2 m/s, substantial variations in velocity occur, with velocities reaching up to 0.7 m/s in the constricted segments. These velocity differences contribute substantially to the formation of vortex structures, which are particularly evident in the outlet area, on top of the packing section. However, the flow stabilizes further downstream, which is not depicted in the section shown. Smaller vortices can also be observed within the packing. Furthermore, a considerable part of the fluid flows past the exterior of the packing between the packing and the cylindrical wall. The augmentation of the cylinder diameter, which is imperative for convergence reasons of the adjoint equation system, exerts a substantial influence on the flow behavior. However, it is noteworthy that the optimization process remains effective. Despite the general resemblance of the structure and velocity fields, it is evident that initial regions exhibiting minimal velocity are being replenished

with material (see black ellipsoid) fostering a more homogeneous fluid distribution in the cross-section. Furthermore, a discernible weakening of the vortex structures is apparent following the shape optimization, accompanied by a reduction in dissipation and, consequently, a decrease in pressure drop. This phenomenon is primarily attributable to the rounding of the structural elements, which deflects the fluid flow more gently. Yet it needs to be noted that the obvious bypassing close to the wall is merely affected by the improvements.

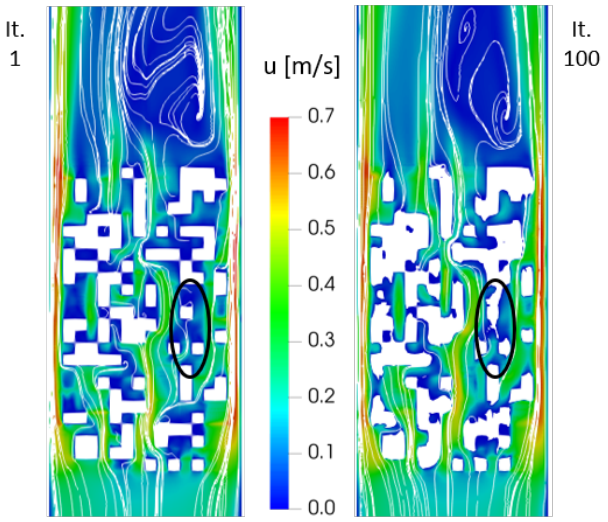

Figure 5. Section of velocity profiles of the initial topology-optimized packing (left) and after 100 shape optimization iterations (right) in central 2D section with streamlines; sections of the cylinder above and below the packing have been removed.

Rombopak packing

The result of the shape optimization of the Rombopak packing is depicted in Figure 5. The development of the pressure drop and the specific surface area over the course of the iterations exhibits a resemblance to the previously studied packing. The specific surface area shows less fluctuation since the geometric constraint is undercut more frequently for this packing. At iteration 49, the specific surface area ceased to exceed the minimum defined value of 499.4 m^2/m^3 and therefore marks the optimum for this packing. The initial pressure drop of 0.036 mbar/m is reduced by 3% whereas the specific surface area remains constant with a negligible deviation of 0.3%.

The initial Rombopak packing and the resulting deformation after 49 shape optimization iterations, depicted in Figure 6, appear rather identical. However, a more thorough examination of the zoomed-in section reveals the deformations of shape optimization. It can be observed that the introduction of new material, particularly in the middle of the structural element and at the joints between different structural elements has been incorporated. Furthermore, as with the topology-optimized packing, the presence of rounded edges is evident. These rounded edges serve to prevent an abrupt change in the direction of fluid flow, thereby preventing flow separation and reducing pressure drop.

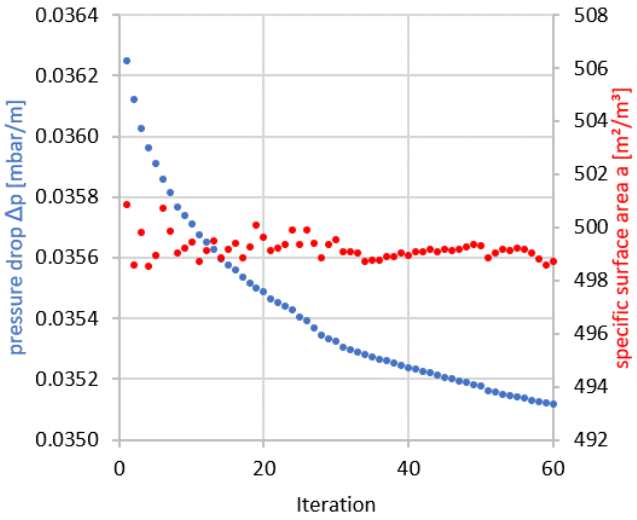

Figure 6. Shape optimization results of the pressure drop and specific surface area for the Rombopak packing.

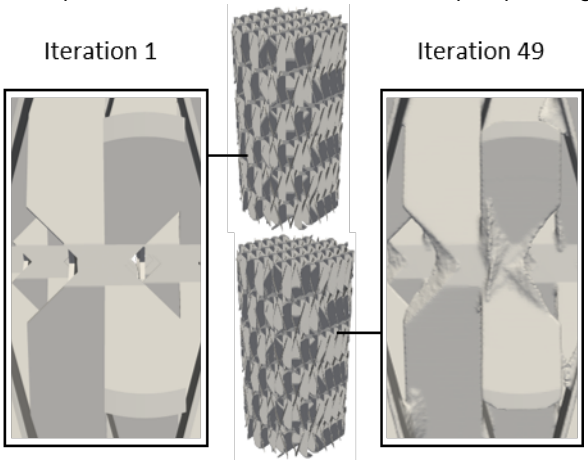

Figure 7. Packing element of the initial Rombopak packing and after 49 shape optimization iteration steps including zoomed-in sections.

An analysis of the velocity profiles and streamlines of the Rombopak packing before and after shape optimization, as shown in Figure 7, reveals more linear streamlines and a more uniform fluid distribution along the cross section compared to the topology-optimized packings, which has a positive effect on the pressure drop. While shape optimization does not significantly affect the velocity plots and streamlines in this case, zoomed-in sections highlight the deformations of the packings. As illustrated in Figure 6, the bottom right ellipse indicates the process of material addition at the joints of structural elements. Furthermore, the top left ellipse demonstrates

that there is an extension of the structural elements in the direction of the flow. An examination of the overall longitudinal section yields the finding that the deformations occur primarily on the outer elements.

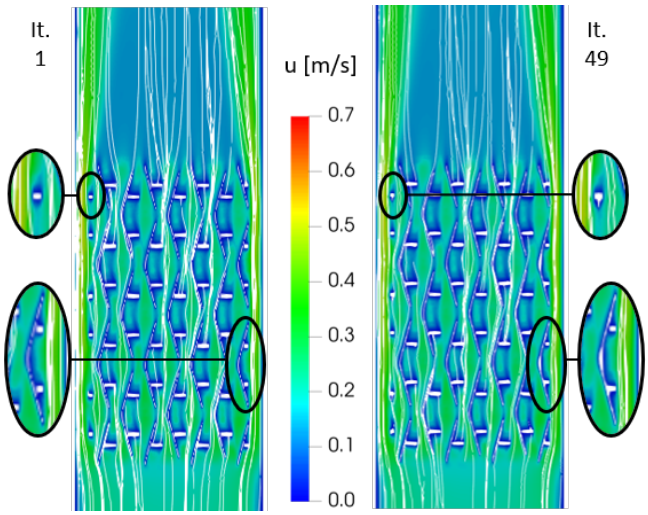

Figure 7. Section of velocity profiles of the initial Rombopak packing (left) and after 49 shape optimization iterations (right) in central 2D section with streamlines with zoomed-in sections; sections of the cylinder above and below the packing have been removed.

CONCLUSION & OUTLOOK

The two optimization studies indicate the successful application of the shape optimization with reduced pressure drop at constant specific surface area. The initial pressure drop of the coarse topology-optimized packing is effectively reduced by 16%, while the pressure drop of the Rombopak packing is reduced only slightly by 3%, and the optimal result was attained after 49 iterations. These differences are however expected due to the coarser structure of the topology-optimized packing, which provides significantly larger potential for improvement. Overall, it can be concluded that shape optimization provides an effective tool for the refinement of existing packing structures.

To further improve the optimization, it is essential to systematically vary the parameterization of the optimization algorithm for every packing considered. A particular emphasis should be placed on the tolerance value for the lower limit of the geometric constraint, as an increase in this value may contribute to a higher freedom for deformation. In order to ascertain the impact of shape deformation on the separation efficiency, experiments of the optimized packings in a distillation column are imperative.

ACKNOWLEDGEMENTS

Funded by the Deutsche Forschungsgemeinschaft (DFG, German Research Foundation) – 544956881.

REFERENCES

1. L. Spiegel, W. Meier. Distillation columns with structured packings in the next decade. *Chem. Eng. Res. Des.* 81:39-47 (2003) https://doi.org/10.1205/026387603321158177
2. J. Neukäufer, F. Hanusch, M. Kutscherauer, S. Rehfeldt, H. Klein, T. Grützner. Methodology for the development of additively manufactured packings in thermal separation. *Chem. Eng. Technol.* 42:1970-1977 (2019) https://doi.org/10.1002/ceat.201900220
3. D. Zawadzki, M. Blazkiewicz, M. Jaskulski, M. Piątkowski, J. Koop, R. Loll, A. Górak. Design and Optimisation of Structural Packings for Rotating Bed Absorbers Using Computational Fluid Dynamics Simulation. *Chem. Eng. Res. Des.* 195:508-525 (2023) https://doi.org/10.2139/ssrn.4222640
4. A. Lange, G. Fieg. Designing novel structured packings by topology optimization and additive manufacturing. *Comp. Aided Chem. Eng.* 49:1291-1296 (2020) https://doi.org/10.1016/B978-0-323-85159-6.50215-3
5. S. Blauth, D. Stucke, M. A. Ashour, J. Schnebele, T. Grützner, C. Leithäuser. CFD-based shape optimization of structured packings for enhancing separation efficiency in distillation. *Chem. Eng. Sci.* 302:120803 (2025) https://doi.org/10.1016/j.ces.2024.120803
6. J. Neukäufer, M. A. Ashour, N. Sarajlic, H. Klein, S. Rehfeldt, H. Hallmann, S. Meinicke, J. Paschold, C. Knösche, T. Grützner. Development of enhanced three-dimensional printed packings for scale-up of distillation columns: a successful case study. *AIChE J.* 69:e17902 (2022) https://doi.org/10.1002/aic.17902
7. C. Othmer. A continuous adjoint formulation for the computation of topological and surface sensitivities of ducted flows. *Int. J. Numer. Meth. Fluids* 58:861-877 (2008) https://doi.org/10.1002/fld.1770